

## **I-1. PROJECT RESEARCHES**

### **Project 8**

## PR8 Project Research on Advances in Isotope-Specific Studies Using Multi-Element Mössbauer Spectroscopy

M. Seto

*Institute for Integrated Radiation and Nuclear Science,  
Kyoto University*

### OBJECTIVES AND PERFORMED RESEARCH SUBJECTS:

The main objectives of this project research are the investigation of the fundamental properties of new materials and the development of the advanced experimental methods by using multi-element Mössbauer spectroscopy. One of the most irreplaceable features of the Mössbauer spectroscopy is to extract element-specific or isotope-specific information. As the Mössbauer resonance line is extremely narrow, hyperfine interactions are well resolved and give us the information on the surrounding electronic states and magnetism. Therefore, promotion of the variety of Mössbauer isotope provides more useful and valuable methods for modern precise materials science of complex systems, such as biological substances, multi-layer films, and complicated-structured matter.

In this project research, each group performed their research by specifying a certain isotope:

$^{57}\text{Fe}$  in P8-1, P8-2, P8-3 and P8-4

$^{119}\text{Sn}$  in P8-5

$^{119}\text{Sn}$  and  $^{151}\text{Eu}$  in P8-6

$^{197}\text{Au}$  in P8-7 and P8-8

Development for other isotopes in P8-9

The subjects of research are as follows:

P8-1 Analysis of iron-based products using Mössbauer spectroscopy – iron oxide scale generated in the boiler feed-water in thermal power plant – (Y. Akiyama *et al.*)

P8-2 EFG tensor of  $\text{Fe}^{2+}$  in M2 site of orthopyroxene by single crystal Mössbauer microspectroscopy (K. Shinoda *et al.*)

P8-3 Temperature dependence of Mössbauer spectra for  $\text{Fe}_2\text{O}_3\text{-Al}_2\text{O}_3$  solid solution (S. Takai *et al.*)

P8-4 A nuclear resonance vibrational spectroscopic study of oxy-myoglobin (Y. Yamamoto *et al.*)

P8-5 Mössbauer spectroscopy on the antiperovskite oxide superconductor  $\text{Sr}_{3-x}\text{SnO}$  (Y. Maeno *et al.*)

P8-6 Researches on magnetism in a novel Kondo lattice (Y. Kamihara *et al.*)

P8-7 Study on structure of gold complexes coordinated with  $\alpha$ -amino acids by means of  $^{197}\text{Au}$  Mössbauer spectroscopy (H. Murayama *et al.*)

P8-8  $^{197}\text{Au}$  Mössbauer study of supported Au nanoparticles catalysis II (Y. Kobayashi *et al.*)

P8-9 Development of Mössbauer spectroscopy for  $^{166}\text{Er}$  (S. Kitao *et al.*)

### MAIN RESULTS AND CONTENTS OF THIS REPORT:

Y. Akiyama *et al.* (P8-1) investigated iron oxide scales generated in the pipe of the boiler feed-water system in the thermal power plant with oxygenated treatment. The information of chemical components of the iron oxide resolved by Mössbauer spectroscopy is necessary for magnetic separation system to remove the scales.

K. Shinoda *et al.* (P8-2) have developed Mössbauer microspectrometer and applied it to the studies of M2 site of orthopyroxene in a crystallographically-oriented enstatite crystal. The EFG tensor of the  $\text{Fe}^{2+}$  at the M2 site was successfully determined.

S. Takai *et al.* (P8-3) studied temperature dependence of  $(\text{Fe}_2\text{O}_3)_{1-x}(\text{Al}_2\text{O}_3)_x$  solid solutions with  $x = 0.5$  by Mössbauer spectroscopy. The temperature dependence of the spectra apparently showed a spectral change due to thermally distributed spin interaction with an effect of small particle size.

T. Ohta and Y. Yamamoto *et al.* (P8-4) have been investigating on oxymyoglobin through vibrational studies to reveal the relationship between the function and the conformation of Fe-O<sub>2</sub> bond in oxymyoglobin.

Y. Maeno *et al.* (P8-5) studied antiperovskite oxide superconductors  $\text{Sr}_{3-x}\text{SnO}$ . Temperature dependence of  $^{119}\text{Sn}$  Mössbauer spectra of  $\text{Sr}_{3-x}\text{SnO}$  ( $x \sim 0.5$ ) have revealed the presence of  $\text{Sn}^{4+}$  site and a site of  $\text{Sn}^{4+}$  hole-doped by Sr deficiency.

Y. Kamihara *et al.* (P8-6) have studied magnetic phases in novel Kondo Lattice,  $\text{EuSn}_2\text{As}_2$  through  $^{151}\text{Eu}$  and  $^{119}\text{Sn}$  Mössbauer spectroscopies. Temperature dependences clearly showed the magnetic splitting below 20K both in Eu and Sn spectra.

H. Murayama *et al.* (P8-7) investigated gold complexes coordinated with amino acids by  $^{197}\text{Au}$ -Mössbauer spectroscopy and obtained the characterization of Au(III) and Au(I) components. This information is helpful for producing Au nanoparticles deposited on various supports.

Y. Kobayashi *et al.* (P8-8) applied  $^{197}\text{Au}$ -Mössbauer spectroscopy to the studies on Au nanoparticles catalysis supported with Hydroxyapatite. The comparison of the catalysis prepared by several calcination temperatures showed a slight effect by this treatment.

S. Kitao *et al.* (P8-9) have developed Mössbauer sources for several less-common Mössbauer spectroscopy. As for source materials of  $^{166}\text{Er}$ -Mössbauer spectroscopy, improvement of source activity in  $\text{HoAl}_2$  was successfully confirmed. This source is useful for various researches for Er compounds.

# PR8-1 Analysis of Iron-based Products Using Mössbauer Spectroscopy - Iron Oxide Scale Generated in the Boiler Feed-water in Thermal Power Plant -

Y. Akiyama, M. Hiramatsu, K. Akiyama, F. Mishima<sup>1</sup>, S. Nishijima<sup>1</sup>, H. Okada<sup>2</sup>, N. Hirota<sup>2</sup>, T. Yamaji<sup>3</sup>, H. Matsuura<sup>3</sup>, S. Namba<sup>3</sup>, T. Sekine<sup>4</sup>, Y. Kobayashi<sup>5</sup>, M. Seto<sup>5</sup>

Graduate School of Engineering, Osaka University

<sup>1</sup> Department of Nuclear Technology and Applied Engineering, Fukui University of Technology

<sup>2</sup> National Institute for Materials Science

<sup>3</sup> Shikoku Research Institute Inc.,

<sup>4</sup> Ebara Industrial Cleaning Co., Ltd.,

<sup>5</sup> Institute for Integrated Radiation and Nuclear Science, Kyoto University

**INTRODUCTION:** One of the reasons for deterioration of power generation efficiency of the thermal power generation is adhesion of the iron oxide scale generated by the corrosion of the pipe to the inner wall of the boiler feed-water system. Focusing on the magnetic properties of the scale, we have studied the removal of scales in the feed-water system by high gradient magnetic separation (HGMS) using the superconducting magnet. In this study, we targeted the thermal power plants adopting oxygenated treatment (OT). In order to determine the installation site and the magnetic separation conditions of the HGMS system, we analyzed the composition of the actual OT scale, which is considered to be the mixture of several kinds of iron oxides, by Mössbauer spectrometry.

**EXPERIMENTS:** The scale was sampled at 6 sampling points in the feed-water system of the power plant adopting OT. The composition was analyzed with Mössbauer spectrometry, and magnetization was analyzed by a physical property measurement system (Quantum Design Inc.). Fig. 1. shows the sampling points in the feed-water system of the thermal power plant. The sampling points were as follows; (1) outlet of condensate pump, (2) outlet of condensate demineralize, (3) drain of low-pressure feed-water heater, (4) inlet of deaerator, (5) storage tank of deaerator and (6) inlet of the economizer.

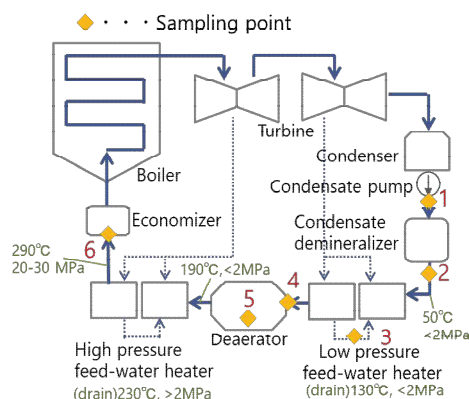


Fig. 1. The sampling points in the feed-water system of the thermal power generation [1].

**RESULTS:** Fig. 2. show the composition of the actual scales at 6 sampling points, respectively. The peaks were clearly separated from the Mössbauer spectrum, indicating that composite crystals may not exist. 6 major components; magnetite ( $\text{Fe}_3\text{O}_4$ ), maghemite ( $\gamma\text{-Fe}_2\text{O}_3$ ), hematite ( $\alpha\text{-Fe}_2\text{O}_3$ ), goethite ( $\alpha\text{-FeOOH}$ ) and lepidocrocite ( $\gamma\text{-FeOOH}$ ) were found in the scale. The composition of the scale was different depending on the sampling points. The scale sampled from the low-pressure feed-water heater drain (LPD) most contained the ferromagnetic magnetite and maghemite, compared with the scales of other sampling points. The sample also showed the highest magnetic susceptibility.

As a next step, the aggregation states of the ferromagnetic and the paramagnetic particles were investigated by lab-scale magnetic separation experiments by superconducting magnet. The experiments were conducted both for the actual scale sampled at low-pressure feed-water heater drain and the simulated sample by mixing commercially available iron oxide and hydroxide according to the result of Fig. 2. The result of the magnetic separation experiment showed that the capture rates showed similar results in actual and simulated scale, indicating the aggregation states of the particles in the simulated and the actual scale were similar. It was also shown that homogeneous aggregation existed in the OT scale, because a part of the paramagnetic particles were captured even in the separation conditions that the pure paramagnetic particles cannot be captured. Based on the results, we are currently designing HGMS system for removing the OT scale.

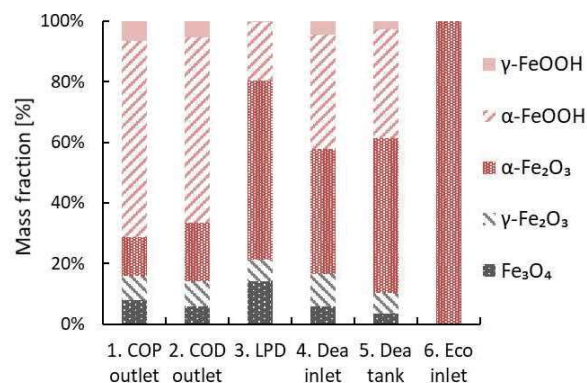


Fig. 2. The composition of the actual scales at 6 sampling points estimated by Mössbauer spectrometry [1].

**Acknowledgments:** This work is partly supported by Advanced Low Carbon Technology Research and Development Program (ALCA) of JST Strategic Basic Research Programs (JPMJAL1304).

## REFERENCES:

[1] M. Hiramatsu *et al.*, J. Phys. Conf. Ser., **1293** (2019) 012079.

K. Shinoda and Y. Kobayashi<sup>1</sup>

Department of Geosciences,  
Graduate School of Science, Osaka City University

<sup>1</sup>Institute for Integrated Radiation and Nuclear Science,  
Kyoto University

**INTRODUCTION:** <sup>57</sup>Fe Mössbauer spectroscopy has been widely used for the analysis of Fe in Fe-bearing minerals. Powdered mineral is generally used as a Mössbauer sample, in spite of the usefulness of the conventional method, it is not useful for the Mössbauer analysis of any narrow area in a crystal or mineral grain. To overcome the disadvantage of spatial resolution by powder method, several Mössbauer microspectrometers have been proposed. Mössbauer microspectroscopy will be widely used for measuring spectra of a grain in a thin section in future. Intensities of component peaks in a quadrupole doublet of a thin section as a single crystal are asymmetric and vary depending on the angle between the direction of incident  $\gamma$ -rays and the crystallographic orientation of the thin section. Intensity of quadrupole doublet ( $I^h / I^{total}$ ) means a ratio between area of the peak of the higher energy ( $I^h$ ) and total area of the doublet ( $I^{total} = I^h + I^l$ ) (sum of  $I^h$  and area of the lower energy ( $I^l$ )). The intensity of component peaks of a <sup>57</sup>Fe Mössbauer doublet is related to an electronic field gradient (EFG) tensor of the site containing Fe<sup>2+</sup> and Fe<sup>3+</sup> (Zimmermann, 1975 and 1983). Thus, EFG determination is important in Mössbauer measurements of thin section as a single crystal. Zimmermann (1975, 1983) introduced experimental determination of EFG tensor from the Mössbauer spectrum of a single crystal, and proposed a formulation of the EFG tensor from the intensities of the component peaks of asymmetric Mössbauer doublet.

In pyroxene, Fe<sup>2+</sup> in M1, Fe<sup>2+</sup> in M2 and Fe<sup>3+</sup> in M1 sites are possible. As three doublets overlap in Mössbauer spectrum of pyroxene, it is important to reveal EFG of three doublets to analyze Mössbauer spectrum of pyroxene thin section. Tennant *et al.* (2000) revealed the EFG tensor of Fe<sup>2+</sup> at the octahedral M1 site of clinopyroxene. Shinoda and Kobayashi (2019) revealed EFG the tensor due to Fe<sup>3+</sup> in M1 site of clinopyroxene. In this study, Zimmermann's method was applied for single crystal <sup>57</sup>Fe Mössbauer spectra of an enstatite crystal on oriented thin sections to determine the EFG tensor of Fe<sup>2+</sup> at the M2 site of *Pbca* orthopyroxene of orthorhombic crystal system. Chemical formula of this sample was (Mg<sub>2.03</sub>, Fe<sub>0.16</sub>)(Si<sub>1.78</sub>, Al<sub>0.13</sub>)O<sub>6</sub> by EDS analyses.

**EXPERIMENTS and RESULTS:** A single crystal of enstatite from Turiani, Morogoro, Tanzania was used for this study. Three crystallographically oriented thin sections which are perpendicular to  $a^*$ ,  $b^*$  and  $c^*$  were prepared by measuring X-ray diffraction using precession camera. Nine Mössbauer spectra of oriented thin sections were measured. In this study, Cartesian coordinate ( $X Y Z$ ) is set as  $X//c^*$ ,  $Y//a^*$ ,  $Z//b^*$ , where  $a^*$ ,  $b^*$ ,  $c^*$  are reciprocal lattice vectors of enstatite. Mössbauer measurements were carried out in transmission mode on a constant acceleration spectrometer with an Si-PIN semiconductor detector (XR-100CR, AMPTEK Inc.) and multi-channel analyzer of 1024 channels. A 3.7GBq <sup>57</sup>Co/Rh of 4mm $\phi$  in diameter was used as  $\gamma$ -ray source. An <sup>57</sup>Fe-enriched iron foil was used as velocity calibrant. The two symmetric spectra were folded and velocity range was  $\pm 5$ mm/s. Thickness corrections of raw spectra were not done.

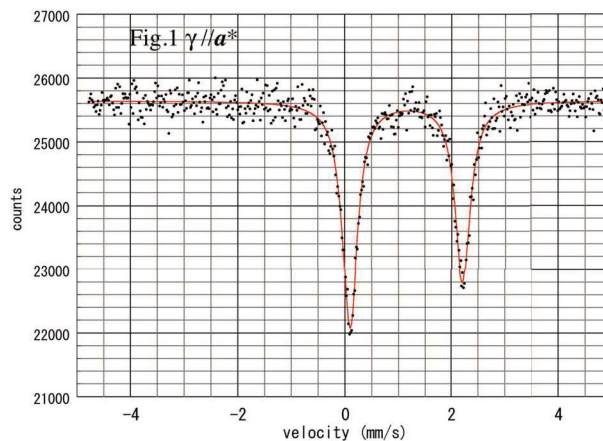


Fig.1 shows representative Mössbauer spectrum of enstatite measured under incident  $\gamma$ -ray parallel to  $a^*$ -axis. A doublet due to Fe<sup>2+</sup> in M2 site of orthopyroxene was observed. Isomer shift, Q-splitting, and line width were 1.06 2.11 and 0.34 mm/s, respectively. From nine sets of intensity of quadrupole doublet, three components of traceless tensor were calculated as 0.116, -0.045 and -0.075. Asymmetric parameter  $\eta$  was 0.266.

#### REFERENCES

- [1] R. Zimmermann (1983) Advances in Mössbauer spectroscopy (Thosar, B.V. Ed.). pp.273-315, Elsevier Scientific Publishing Co. Amsterdam.
- [2] R. Zimmermann (1975) Nucl. Instr. and Meth. **128**, 537-543.
- [3] W.C. Tennant, C. A. McCammon and R. Miletich (2000) Phys. Chem. Min., **27**, 156-163.
- [4] K. Shinoda, Y. Kobayashi (2019) J. Min. Petro. Sci., **114**, 130-141.

## PR8-3 Temperature Dependence of Mössbauer Spectra for Fe<sub>2</sub>O<sub>3</sub>-Al<sub>2</sub>O<sub>3</sub> Solid Solution

S. Takai<sup>1</sup>, H. Nakaishi<sup>1</sup>, K. Ota<sup>1</sup>, T. Yabutsuka<sup>1</sup>, T. Yao<sup>2</sup>, S. Kitao<sup>3</sup>, M. Seto<sup>3</sup>

<sup>1</sup>Graduate School of Energy Science, Kyoto University

<sup>2</sup>Kyoto University

<sup>3</sup>Institute for Integrated Radiation and Nuclear Science, Kyoto University

**INTRODUCTION:** Although both  $\alpha$ -Fe<sub>2</sub>O<sub>3</sub> and  $\alpha$ -Al<sub>2</sub>O<sub>3</sub> possess corundum-type structure, the solid solution range is so restricted as approximately 10 % from the terminal compositions due to 5.6 % smaller *c*-length for Al<sub>2</sub>O<sub>3</sub> in comparison with Fe<sub>2</sub>O<sub>3</sub> [1]. We have recently revealed that corundum-type structured solid solution can be obtained in the hole compositional range of Fe<sub>2</sub>O<sub>3</sub>-Al<sub>2</sub>O<sub>3</sub> system by means of mechanochemical method using high-energy ball milling technique. In terms of the continuous substitution of non-magnetic aluminum ions instead of iron in Fe<sub>2</sub>O<sub>3</sub>, dilution of spin interaction can be achieved in corundum-type structure, which would result in the variation of magnetic properties of (Fe<sub>2</sub>O<sub>3</sub>)<sub>1-x</sub>(Al<sub>2</sub>O<sub>3</sub>)<sub>x</sub> solid solution system.

$\alpha$ -Fe<sub>2</sub>O<sub>3</sub> exhibits antiferromagnetic properties at low temperatures, which undergo Morin transition at 265 K on heating to show a weak ferromagnetic. In the previous study (30121), Mössbauer spectroscopy experiments have been carried out on (Fe<sub>2</sub>O<sub>3</sub>)<sub>1-x</sub>(Al<sub>2</sub>O<sub>3</sub>)<sub>x</sub> solid solutions at room temperature. It is found that the Mössbauer spectra varies from sextet peaks at *x* = 0 into almost doublet at *x* = 0.50. This indicates that substitution of aluminum ions allows the change in magnetic properties from weak ferromagnetism to paramagnetic state by reducing the spin interactions. It is also expected that spin ordering would be attributed by temperature, i.e. the Mössbauer spectra should be altered by reducing temperature. In the present study, we measured the Mössbauer spectra in the temperature range from 4 K up to the room temperature to investigate the variation of magnetic properties of (Fe<sub>2</sub>O<sub>3</sub>)<sub>0.5</sub>(Al<sub>2</sub>O<sub>3</sub>)<sub>0.5</sub>.

**EXPERIMENTS:** Stoichiometric mixture of  $\gamma$ -Fe<sub>2</sub>O<sub>3</sub> and  $\gamma$ -Al<sub>2</sub>O<sub>3</sub> reagents were put into a silicon nitride milling pod with 10 milling balls with the diameter of  $\phi$ 10. In the present study, the compositions were selected as *x* = 0.50 for (Fe<sub>2</sub>O<sub>3</sub>)<sub>1-x</sub>(Al<sub>2</sub>O<sub>3</sub>)<sub>x</sub> system. Mechanical alloying has been carried out using a planetary ball milling machine operated at 800 rpm for 240 min. The crystalline phase of the obtained sample was confirmed by X-ray diffraction.

For the measurement of Mössbauer spectroscopy, <sup>57</sup>Co in Rh was employed as the  $\gamma$ -ray source. Doppler velocity scale has been calibrated by using Fe foil. The Mössbauer spectra were collected at various temperatures below 300K. Low temperature has been achieved by using He gas flow type refrigerator or liquid N<sub>2</sub> cryostat.

**RESULTS:** The Mössbauer spectra measured at various temperatures are represented in Fig. 1. At 300 K,

apparent doublet peaks are observed as the previous investigation of last year (30121). The doublet diminishes with decreasing temperature, while the sextet grows around 200 K, and almost sextet peaks are remained below 40 K. It is supposed that spin interaction thermally disturbed and attributed by small particle size would bring about the ordering at lower temperatures. Further precise analysis is now carried out accompanied by the neutron diffraction. Moreover, additional low temperature Mössbauer experiments are planning with other compositions.

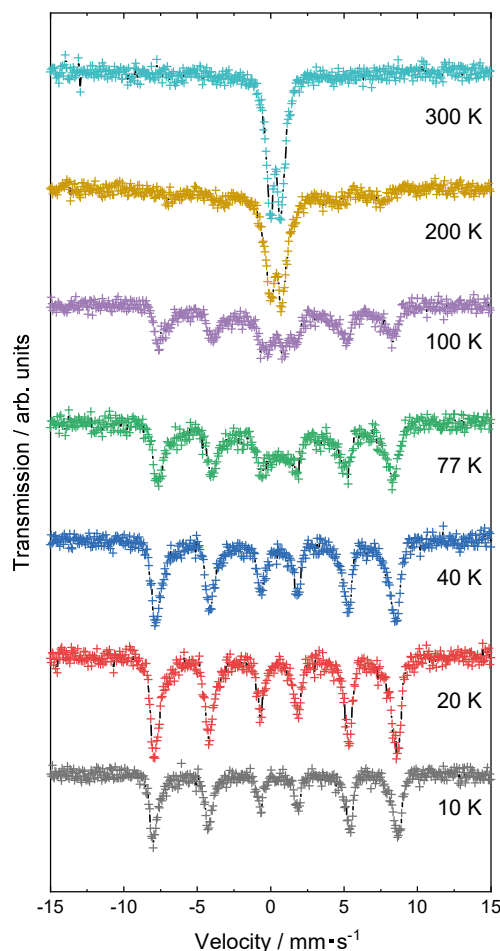


Fig. 1. Temperature dependence of Mössbauer spectra for (Fe<sub>2</sub>O<sub>3</sub>)<sub>0.5</sub>(Al<sub>2</sub>O<sub>3</sub>)<sub>0.5</sub>.

### REFERENCES:

- [1] A. Muan *et al.*, *J. Am. Ceram. Soc.*, 39 (1956) 207-214.
- [2] S. Takai *et al.*, *Solid State Ionics*, 313 (2017) 1-6.

## PR8-4 A Nuclear Resonance Vibrational Spectroscopic Study of Oxy Myoglobin

T. Ohta, T. Shibata<sup>1</sup>, M. Saito<sup>2</sup>, M. Seto<sup>2</sup>, Y. Kobayashi<sup>2</sup>, S. Yanagisawa<sup>3</sup>, T. Ogura<sup>3</sup>, Y. Yamamoto<sup>1</sup>, S. Neya<sup>4</sup> and A. Suzuki<sup>5</sup>

Department of Applied Chemistry, Faculty of Engineering, Sanyo-Onoda City University

<sup>1</sup>Department of Chemistry, University of Tsukuba

<sup>2</sup>Integrated Radiation and Nuclear Science, Kyoto University

<sup>3</sup>Graduate School of Life Science, University of Hyogo

<sup>4</sup>Graduate School of Pharmaceutical Sciences, Chiba University

<sup>5</sup>Department of Materials Engineering, National Institute of Technology, Nagaoka College

**INTRODUCTION:** Myoglobin (Mb), an oxygen (O<sub>2</sub>) storage hemoprotein, has been served as a paradigm for the structure-function relationship of metalloproteins. O<sub>2</sub> is reversibly bound to a ferrous heme Fe atom (Fe(II)) in Mb. Although the reaction between O<sub>2</sub> and heme Fe(II) of Mb is often considered as one of the simplest biological reactions, in fact, the reaction is much more complicated than it appears. Upon oxygenation of the protein, ground state triplet O<sub>2</sub> is bound to a high-spin quintet heme Fe(II) in Mb to yield a low-spin singlet heme Fe(II) in oxy Mb (MbO<sub>2</sub>), which is considered as a mixture of Weiss (Fe<sup>3+</sup>(*S* = 1/2)-O<sub>2</sub><sup>-</sup>(*S* = 1/2)),<sup>1</sup> Pauling (Fe<sup>2+</sup>(*S* = 0)-O<sub>2</sub>(*S* = 0)),<sup>2</sup> and McClure forms (Fe<sup>2+</sup>(*S* = 1)-O<sub>2</sub>(*S* = 1)).<sup>3</sup> We characterized MbO<sub>2</sub>s possessing <sup>57</sup>Fe-enriched heme cofactors (Figure 1) using nuclear resonance vibrational spectroscopy (NRVS) to elucidate the electronic nature of the Fe-O<sub>2</sub> bond.<sup>4</sup>

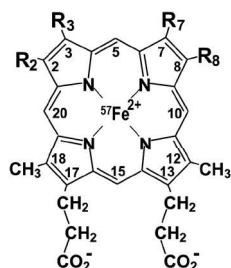


Figure 1. The structures and numbering system for the heme cofactors used in the study. Proto (R<sub>2</sub> = R<sub>7</sub> = CH<sub>3</sub>, R<sub>3</sub> = R<sub>8</sub> = CH=CH<sub>2</sub>), Meso (R<sub>2</sub> = R<sub>7</sub> = CH<sub>3</sub>, R<sub>3</sub> = R<sub>8</sub> = C<sub>2</sub>H<sub>5</sub>), and 7-PF (R<sub>2</sub> = CH<sub>3</sub>, R<sub>3</sub> = R<sub>8</sub> = C<sub>2</sub>H<sub>5</sub>, R<sub>7</sub> = CF<sub>3</sub>).

**EXPERIMENTS:** Iron-<sup>57</sup>Fe (95 atom%, Merck) was used to prepare <sup>57</sup>Fe-enriched heme cofactors. Sperm whale Mb was purchased as a lyophilized powder from Biozyme and used without further purification. Apoprotein of Mb was prepared using the procedure of Teale<sup>5</sup>. <sup>57</sup>Fe-enriched Proto, Meso, and 7-PF (Figure 1) were incorporated into apoprotein, and then the obtained proteins were converted to oxy forms, i.e., MbO<sub>2</sub>(Proto), MbO<sub>2</sub>(Meso), and MbO<sub>2</sub>(7-PF), respectively, using the standard procedure. NRVS measurements were performed at SPring-8, BL09XU<sup>6</sup>. During the data collection, the protein samples were maintained at low temperature using a liquid He cryostat (head temperature <10 K). Spectra were recorded between -20 and 80 meV in 0.25 meV steps. <sup>57</sup>Fe partial vibrational density of states (<sup>57</sup>Fe PVDOS) was calculated using a program PHOENIX<sup>7</sup>.

**RESULTS:** Based on the <sup>57</sup>Fe PVDOS of the proteins (Figure 2A), we found that the vibrational spectrum of MbO<sub>2</sub>(Proto) can be better reproduced by the spin polarized Fe<sup>3+</sup>-O<sub>2</sub><sup>-</sup> state calculated on the basis of broken-symmetry singlet state, rather than the Fe<sup>2+</sup>-O<sub>2</sub> closed-shell singlet one, in terms of the vibrational energies and peak intensities of the major bands due to the Fe-O<sub>2</sub> bond and the bonds between heme Fe and pyrrole nitrogen atoms. This finding supported the dominance of the Weiss form<sup>1</sup> in the nature of the Fe-O<sub>2</sub> bond in the protein.

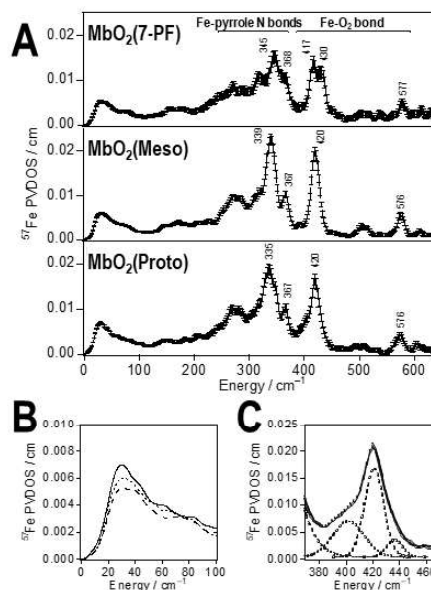


Figure 2. <sup>57</sup>Fe PVDOS of MbO<sub>2</sub>(Proto) at 43 K (bottom), MbO<sub>2</sub>(Meso) at 27 K (middle) and MbO<sub>2</sub>(7-PF) at 26 K (top) (A), expanded <sup>57</sup>Fe PVDOS of MbO<sub>2</sub>(Proto) (solid line), MbO<sub>2</sub>(Meso) (dotted line) and MbO<sub>2</sub>(7-PF) (broken line) in 0–100 cm<sup>-1</sup> (B), and deconvolution of Fe-O<sub>2</sub> band region, 370–470 cm<sup>-1</sup>, of MbO<sub>2</sub>(Proto) (C).

The comparison of the <sup>57</sup>Fe PVDOS below 100 cm<sup>-1</sup> between the proteins (Figure 2B) indicated that translational motion of heme cofactor is larger in MbO<sub>2</sub>(Proto) compared with those in MbO<sub>2</sub>(Meso) and MbO<sub>2</sub>(7-PF). The large conformational flexibility of MbO<sub>2</sub>(Proto) would be due to the presence of multiple conformations of the Fe-O<sub>2</sub> bond, because deconvolution of the Fe-O<sub>2</sub> band region of the <sup>57</sup>Fe PVDOS of MbO<sub>2</sub>(Proto), i.e., 400–430 cm<sup>-1</sup>, yielded at least three peaks at 402, 421 and 436 cm<sup>-1</sup> (Figure 2C), indicative of the presence of multiple conformations.

### REFERENCES:

- [1] J. J. Weiss, *Nature*, **202**, 83-84 (1964).
- [2] L. Pauling, *Nature*, **203**, 182-183 (1964).
- [3] D. S. McClure, *Radiation. Res. Suppl.*, **2**, 218-242 (1960).
- [4] T. Ohta *et al.*, *Biochemistry*, **57**, 6649-6652 (2018).
- [5] F. W. J. Teale, *Biochim. Biophys. Acta*, **35**, 543 (1959).
- [6] Y. Yoda *et al.*, *Hyperfine Interact.*, **206**, 83-86 (2012).
- [7] J. T. Sage *et al.*, *J. Phys.: Condens. Matter.*, **13**, 7707–7722 (2001).

Y. Maeno, M. Seto<sup>1</sup>, S. Kitao<sup>1</sup>, S. Yonezawa, A. Ikeda,  
S. Koibuchi, and M. Oudah.<sup>2</sup>

Graduate School of Science, Kyoto University

<sup>1</sup>Institute for Integrated Radiation and Nuclear Science,  
Kyoto University

<sup>2</sup>Stewart Blusson Quantum Matter Institute, University of  
British Columbia

**INTRODUCTION:** Antiperovskite (inverse perovskite) oxides  $A_3BO$  ( $A$ : group-2 element,  $B$ : group-14 element) crystallize in the same structure as the ordinary perovskite oxides, but with inverted positions of the cations and anions [1]. In those materials, a metallic anion  $B^{4-}$  ( $\text{Sn}^{4-}$ ,  $\text{Pb}^{4-}$ , etc.) is expected to satisfy the charge neutrality, assuming the ionic states of  $A^{2+}$  and  $\text{O}^{2-}$ . Metallic anions are rare especially in oxides. Originating from the unusual oxidation state, antiperovskite oxides are candidates for topological crystalline insulators [2, 3]. In 2016, some of the present authors discovered the first superconductor among antiperovskite oxides,  $\text{Sr}_{3-x}\text{SnO}$  [4]. Reflecting the nontrivial topology in the normal state, topological superconductivity is theoretically possible in this compound [5]. To investigate the unusual properties of this material, we performed Mössbauer spectroscopy on the Sn nucleus.

**EXPERIMENTS:** The sample was prepared from Sr (Sigma-Aldrich, 99.99%) and SnO (Sigma-Aldrich 99.99%) using the reaction  $(3-x)\text{Sr} + \text{SnO} \rightarrow \text{Sr}_{3-x}\text{SnO}$ , with a condition of  $x \sim 0.5$  [6]. From powder x-ray diffraction, we confirmed that the sample is dominated by  $\text{Sr}_{3-x}\text{SnO}$ . Superconductivity with a volume fraction of about 10% was observed below 5 K in a magnetization measurement. We also observed superconductivity of  $\beta$ -Sn impurity. From the diamagnetic signal, we estimated the amount of  $\beta$ -Sn impurity to be 14 mol %. We conducted Mössbauer spectroscopy at the Institute for Integrated Radiation and Nuclear Science, Kyoto University.  $^{119\text{m}}\text{Sn}$  in the form of  $\text{CaSnO}_3$  (Ritverc GmbH, 740 MBq) was used as the  $\gamma$ -ray source.

**RESULTS:** We present the Mössbauer spectra of  $\text{Sr}_{3-x}\text{SnO}$  in Fig. 1. We observed a clear  $\gamma$ -ray absorption with a shoulder at high temperatures, and the relative intensity of the shoulder increases at low temperatures.

To analyze the data, we fitted the spectra with three Lorentz functions, corresponding to the main and shoulder absorptions as well as  $\beta$ -Sn impurity. The isomer shift and intensity of one of three Lorentzians were fixed to that of the reported value for  $\beta$ -Sn and 14%, respectively. As a result, the isomer shifts at 3 K are fitted to be 1.960(6) mm/s for the main absorption and 2.973(11) mm/s for the shoulder. Since the isomer shift of the main absorption is close to that of  $\text{Mg}_2\text{Sn}$ , in which  $\text{Sn}^{4-}$  is anticipated, this result evidences presence of  $\text{Sn}^{4-}$  in

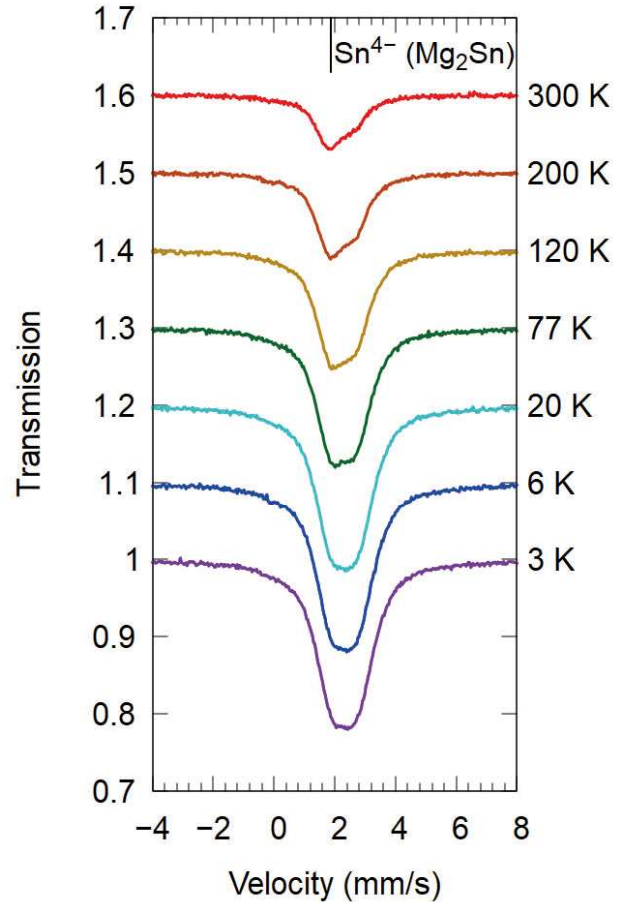


Fig. 1. Mössbauer spectra of  $\text{Sr}_{3-x}\text{SnO}$  ( $x \sim 0.5$ ) with respect to the isomer shift of  $\text{BaSnO}_3$ . Each spectrum is shifted upward by 0.1 for visibility.  $\gamma$ -ray absorption with an isomer shift similar to that of  $\text{Mg}_2\text{Sn}$  evidences presence of  $\text{Sn}^{4-}$ . In addition, another absorption with a larger isomer shift originating from Sr deficiency was observed.

$\text{Sr}_{3-x}\text{SnO}$ . The shoulder with a larger isomer shift originates from a modified ionic state of  $\text{Sn}^{4-}$  hole-doped by Sr deficiency. The greater temperature evolution of the shoulder, corresponding to a higher local Debye temperature, is consistent with the Sn atoms neighboring the Sr vacancies.

Detailed results were published in Ref. [6], where we evaluated the isomer shift and the Debye temperature using the first-principles calculation.

#### REFERENCES:

- [1] A. Widera and H. Schafer, *Mater. Res. Bull.* **15** (1980) 1805–1809.
- [2] T. Kariyado and M. Ogata, *J. Phys. Soc. Jpn.* **80** (2011) 083704.
- [3] T. H. Hsieh *et al.*, *Phys. Rev. B* **90** (2014) 081112(R).
- [4] M. Oudah *et al.*, *Nat. Commun.* **7** (2016) 13617.
- [5] T. Kawakami *et al.*, *Phys. Rev. X* **8** (2018) 041026.
- [6] A. Ikeda *et al.*, *Phys. Rev. B* **100** (2019) 245145.

Y. Kamihara, R. Sakagami, S. Kitao<sup>1</sup>, M. Seto<sup>1</sup>

Department of Applied Physics and Physico-Informatics,  
Keio University

<sup>1</sup>Institute for Integrated Radiation and Nuclear Science,  
Kyoto University

**INTRODUCTION:** In this research, we demonstrate the magnetic phases in a novel Kondo lattice,  $\text{EuSn}_2\text{As}_2$ .  $\text{EuSn}_2\text{As}_2$  is an inter-metallic compound, which is reported by Arguilla *et al.*[1] and is a 2 dimensional layered magnetic compound composed by Eu cation and negative charged  $\text{Sn}_2\text{As}_2$ . In a unit cell of  $\text{EuSn}_2\text{As}_2$ , van der Waals interaction is dominant force to make chemical bonding along  $c$ -axis. Such characteristic chemical bonds are similar to those of "state of art" 2 dimensional topological insulator,  $\text{Bi}_2(\text{Se}, \text{Te})_3$  [2,3,4], which have been focused as thermo electric materials since 1961 or earlier. In 2019, we unveiled a complex magnetic phases in  $\text{EuSn}_2\text{As}_2$ .

In undoped  $\text{EuSn}_2\text{As}_2$ , density functional theory (DFT) demonstrates that a sublattice of Eu orders antiferromagnetically at temperature ( $T$ ) = 0 K, although Eu ions ferromagnetically ordered along  $a / b$  axes; i.e. the Eu orders ferromagnetic intra layer.

In 2019, we demonstrated spontaneous magnetic moments of undoped  $\text{EuSn}_2\text{As}_2$  using DC-magnetic moment measurements. The spontaneous magnetic moments verify a ferromagnetic phase of undoped  $\text{EuSn}_2\text{As}_2$  under weak finite magnetic fields at low  $T$ . [5]

These results indicate that a magnetic phase of undoped  $\text{EuSn}_2\text{As}_2$  is changed to the ferromagnetic order under finite magnetic fields from the antiferromagnetic order under a zero field. In the ferromagnetic order phase, the Eu ion exhibits  $\sim 5 \mu_B$  at  $T < \sim 20$  K. The magnetic moment of Eu is smaller than that of representative  $\text{Eu}^{2+}$ .

The small magnetic moment of Eu suggests a highly hybridized electronic orbital among Eu and Sn atomic orbitals, although direct measurements of internal magnetic fields have not been reported for  $\text{EuSn}_2\text{As}_2$ .

In this research, we have measured  $^{151}\text{Eu}$  and  $^{119}\text{Sn}$  Mössbauer spectroscopy, and demonstrate an appearance of internal magnetic fields at low  $T$  in undoped  $\text{EuSn}_2\text{As}_2$ .

**EXPERIMENTS:** Synthesis procedure of the polycrystalline undoped  $\text{EuSn}_2\text{As}_2$  has been reported in ref.[6]. Optical systems for the Mössbauer spectroscopy are conventional.[7]

**RESULTS:** As shown in Fig. 1, Mössbauer spectra of  $^{151}\text{Eu}$  demonstrate a clear magnetic splitting at  $T = 4.2$  K for undoped  $\text{EuSn}_2\text{As}_2$ . As shown in Fig. 2, the  $^{119}\text{Sn}$  Mössbauer spectra also demonstrate magnetic splitting at  $T < 20$  K. A quantitative analysis on internal magnetic field should be performed in the collaborative research in 2020.

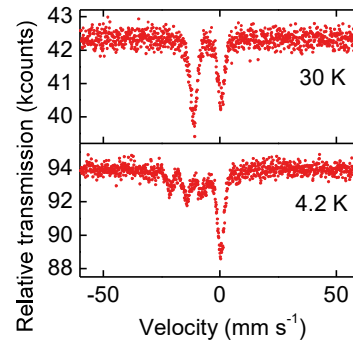


Fig. 1.  $^{151}\text{Eu}$  Mössbauer spectra for polycrystalline undoped  $\text{EuSn}_2\text{As}_2$ .

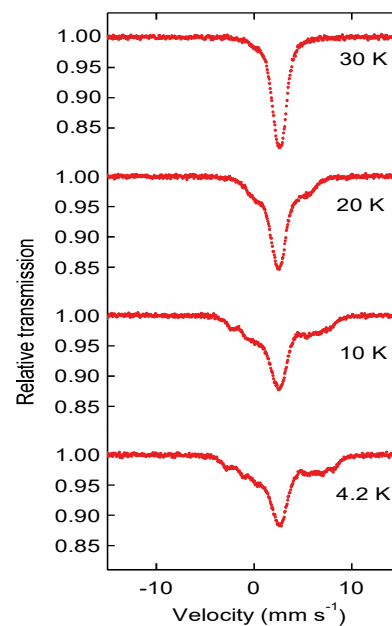


Fig. 2.  $^{119}\text{Sn}$  Mössbauer spectra for polycrystalline undoped  $\text{EuSn}_2\text{As}_2$ .

#### REFERENCES:

- [1] M. Q. Arguilla, *et al.*, Inorg. Chem. Front. 4, 378-386 (2017).
- [2] C. L. Kane and E. J. Mele, Phys. Rev. Lett. 95, 146802 (2005).
- [3] H. Zhang, *et al.*, Nature Phys. 5, 438-442 (2009).
- [4] H. J. Goldsmid and R. T. Delves, G.E.C. Journal 28, 102 (1961).
- [5] K. Hirata, *et al.*, "Spontaneous magnetic polarization of a layered hexagonal compound,  $\text{EuSn}_2\text{As}_2$ ", The 6th Japan-Korean International Symposium on Materials Science and Technology (JKMST2019), Sapporo, Japan: 26th August 2019.
- [6] R. Sakagami, *et al.*, Mater. Sci. Tech. Jpn. 55, 72-76 (2018). In Japanese
- [7] S. Kitao, *et al.*, J. Phys. Soc. Jpn. 77, 103706 (2008).



## PR8-7 Study on Structure of Gold Complexes Coordinated with $\alpha$ -Amino Acids by Means of $^{197}\text{Au}$ Mössbauer Spectroscopy

H. Murayama, M. Takaki, Y. Kobayashi<sup>1</sup>, H. Ohashi<sup>2</sup>, T. Ishida<sup>3</sup>, D. Kawamoto<sup>4</sup> and M. Tokunaga

Department of Chemistry, Kyushu University

<sup>1</sup>Institute for Integrated Radiation and Nuclear Science, Kyoto University

<sup>2</sup>Faculty of Symbiotic Systems Science, Fukushima University

<sup>3</sup>Department of Applied Chemistry for Environment, Tokyo Metropolitan University

<sup>4</sup>Department of Chemistry, Okayama University of Science

**INTRODUCTION:** Gold nanoparticles show catalytic activities when their sizes were less than 5 nm. We have reported a simple and easy impregnation method for the preparation of small gold nanoparticles deposited on various supports [1]. A gold complex coordinated with  $\beta$ -alanine (Au- $\beta$ -ala) was synthesized as a chloride-free and water-soluble precursor for this method. A molecular structure of Au- $\beta$ -ala was determined as mononuclear complexes of  $\text{Au}^{3+}$  with square-planar coordination by means of in situ X-ray absorption fine structure, TG-DTA, and DFT calculations (Fig. 1). Recently, the gold complexes coordinated with various kinds of amino acids were synthesized to realize better precursor than Au- $\beta$ -ala. In this study, the structures of the gold complexes were analyzed by  $^{197}\text{Au}$  Mössbauer spectra.

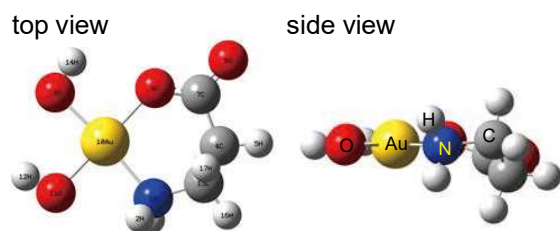


Fig. 1. The geometry of Au- $\beta$ -ala optimized by DFT calculation.

**EXPERIMENTS:** Gold complexes coordinated with amino acid ( $\beta$ -ala,  $\gamma$ -aminobutyric acid (GABA),  $\delta$ -aminovaleric acid (DAVA),  $\epsilon$ -aminocaproic acid (EAHA), tryptophan (Trp), histidine (His), and tyrosine (Tyr)) were synthesized as follows: ethanol was added to a NaOH aqueous solution in which amino acid was dissolved. The amino acid solution was then added to the  $\text{HAuCl}_4$  ethanol/water mixed solution. The mixed solution was left at  $-18^\circ\text{C}$  for 12 h. The precipitates were collected and washed with ethanol/water. The solid was dried to obtain Au-amino acid complex powder [1].  $^{197}\text{Au}$  Mössbauer spectra of the synthesized Au-amino acid complexes were collected at Institute for Integrated Radiation and Nuclear Science, Kyoto University. The  $\gamma$ -ray source ( $^{197}\text{Pt}$ ) feeding the 77.3 keV Mössbauer tran-

sition of  $^{197}\text{Au}$ , was prepared by neutron irradiation of isotopically enriched  $^{196}\text{Pt}$  metal at the Kyoto University Reactor. The  $\gamma$ -ray source and the samples were cooled to a temperature below 20K. The isomer shift ( $IS$ ) of Au foil was referenced to 0 mm/s.

**RESULTS:** As shown in Fig. 2a, the  $^{197}\text{Au}$  Mössbauer spectrum for Au- $\beta$ -ala, which consisted of doublet peaks, was analyzed and then the  $IS$  and the quadrupole splitting ( $QS$ ) were obtained as 4.29 mm/s and 4.93 mm/s, respectively. Similar values were obtained from analyses of the spectra for Au-GABA, Au-DAVA, and Au-EAHA. The values of  $IS$ - $QS$  were in the range of data given by various four-coordinate gold(III) compounds [2]. In addition to the doublet as same as that in the spectrum for Au- $\beta$ -ala, another doublet was observed in the spectrum for Au-Trp (Fig. 2b). The values of  $IS$  and  $QS$  were 3.44 mm/s and 7.83 mm/s, respectively. The characteristic double doublets were also observed in the spectra for gold complexes coordinated with  $\alpha$ -amino acid (His and Tyr) indicating that those gold complexes were mixtures of gold(III) and gold(I).

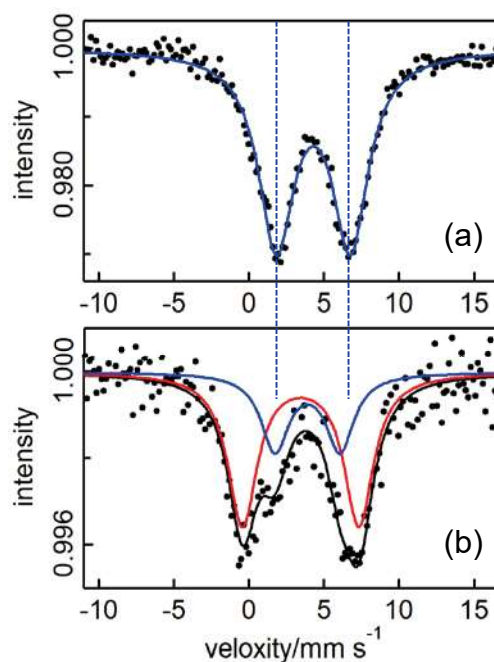


Fig. 2.  $^{197}\text{Au}$  Mössbauer spectra for (a) Au- $\beta$ -ala and (b) Au-Trp.

### REFERENCES:

- [1] H. Murayama *et al.*, J. Catal., **353** (2017) 74-80.
- [2] R. V. Parish, Gold Bull., **15** (1982) 51-63.

Y. Kobayashi, J. Wang<sup>1</sup> and M. Seto

*Institute for Integrated Radiation and Nuclear Science,  
Kyoto University*

<sup>1</sup>*Dalian Institute of Chemical Physics, Chinese Academy  
of Sciences*

**INTRODUCTION:** The normal surface of metallic gold does not adsorb small molecules like hydrogen and oxygen; thus, gold is not generally considered as a good catalyst. Small particles have many edges, corners, and metastable surfaces, and they are different from bulk for catalytic activities. Dispersing the small particles on supports, the catalytic activity of gold increases. Au small particles supported on some materials show high catalytic activity to oxidize CO to CO<sub>2</sub> at temperatures as low as 197K [1,2].

The interaction between particles and supports may give new activity to the catalysts. Hydroxyapatite (HAp) is known as bone mineral, and it is nature friendly. Further-more, it is good support for nanoparticles [3]. HAp binds strongly with Au, and it avoids the fusion of the nanoparticles. This binding with HAp may change the charge of Au, which is expected to show different properties from the bulk.

We have studied the supported Au nanoparticles catalysis using <sup>197</sup>Au Mössbauer spectroscopy. We can observe the signals from Au atoms without disturbance from supports by <sup>197</sup>Au Mössbauer spectroscopy. Moreover, it is sensitive to the electronic states of Au atoms. Thus, Mössbauer spectroscopy is powerful for the study of supported catalysts.

**EXPERIMENTS:** The supported Au nanoparticles catalysis was prepared by the deposition precipitation method and calcination. The mixed solution of HAuCl<sub>4</sub> and HAp was kept on pH 9 and 65°C, thus the Au ions were precipitate on HAp as Au(OH)<sub>3</sub>. After precipitation, the specimens were washed with distilled water, and dried. These specimens were calcined for 4 hours at 200~800°C in air. At that time, Au(OH)<sub>3</sub> was degraded into Au metal, and the Au nanoparticles were firmly fixed on HAp.

<sup>197</sup>Au Mössbauer measurement was conducted using a constant-acceleration spectrometer with a NaI scintillation counter. The <sup>197</sup>Au  $\gamma$ -ray source (77.3 keV) was obtained from <sup>197</sup>Pt (half-life; 18.3 hrs) generated by irradiation of neutron to 98%-enriched <sup>196</sup>Pt metal foil using KUR. The  $\gamma$ -ray source and samples were cooled to 16 K, and the spectra were recorded in a transmission geometry. The isomer shift value of a gold foil was referenced to 0 mm/s.

**RESULTS:** Figure 1 shows the <sup>197</sup>Au Mössbauer spectra of the Au nanoparticle catalysis prepared by several calcination temperatures. All observed spectra show almost the same shape and peak position. This result indicates that the electronic states of the nanoparticles are nearly the same as that of metallic bulk Au. However, in detail, the value of the isomer shift slightly changes from 0.09 mm/s to 0.04 mm/s from the 200°C calcined sample to the 800°C calcined sample. The direction of this change is the direction in which the charge of the Au atom decreases; however, the difference is only slightly above the error, and further verification is necessary.

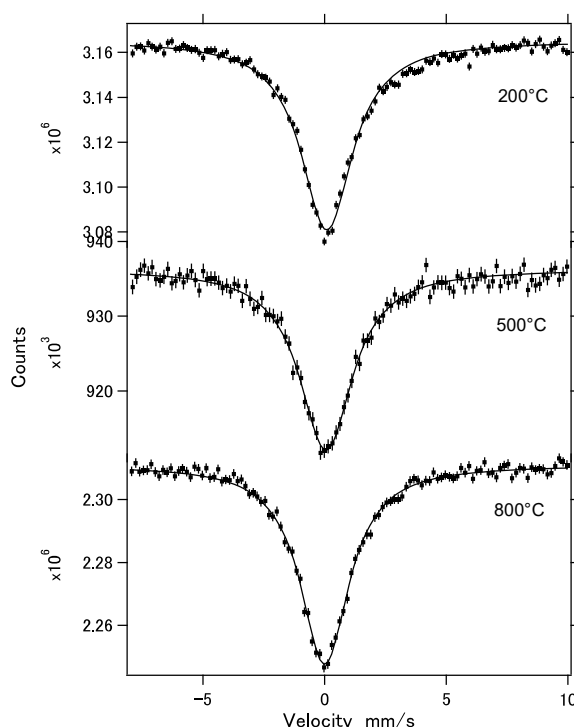


Fig. 1 <sup>197</sup>Au Mössbauer spectra of Au nano-particles catalysis prepared by several calcination temperatures. The measurement temperature was 16K.

**REFERENCES:**

- [1] M. Haruta, T. Kobayashi, H. Sano and N. Yamada, *Chem. Lett.*, **16** (1987) 405.
- [2] M. Haruta, N. Yamada, T. Kobayashi and S. Iijima, *J. Catal.*, **115** (1989) 301.
- [3] Yanjie Zhang, Junhu Wang, Jie Yin, Kunfeng Zhao, Changzi Jin, Yuying Huang, Zheng Jiang, and Tao Zhang, *J. Phys. Chem. C*, **114** (2010) 16443-16450.

S. Kitao<sup>1</sup>, M. Kobayashi<sup>1</sup>, T. Kubota<sup>1</sup>, M. Kurokuzu<sup>1</sup>, H. Tajima<sup>2</sup>, and M. Seto<sup>1</sup>

<sup>1</sup>*Institute for Integrated Radiation and Nuclear Science, Kyoto University*

<sup>2</sup>*Graduate School of Science, Kyoto University*

## INTRODUCTION:

The Mössbauer spectroscopy is one of the most powerful methods for investigation of electronic states, magnetic properties, chemical properties, and so on. A remarkable feature of this method is to extract the information of the specific isotope. Although about one hundred of Mössbauer energy levels are known, research activities in Mössbauer studies so far are quite limited, except  $^{57}\text{Fe}$  and  $^{119}\text{Sn}$ . It is partly because commercially available sources at present are only  $^{57}\text{Co}$  and  $^{119\text{m}}\text{Sn}$  for the Mössbauer spectroscopy of  $^{57}\text{Fe}$  and  $^{119}\text{Sn}$ , respectively.

On the contrary, at the Institute for Integrated Radiation and Nuclear Science, various short-lived isotopes can be obtained by neutron irradiation at Kyoto University Research Reactor(KUR). Moreover, some short-lived isotopes can be complementarily produced by high-energy  $\gamma$ -ray irradiation at the electron linear accelerator(KURNS-LINAC). Thus, we have already been performing Mössbauer spectroscopy with various isotopes(by source nuclides in parentheses):  $^{61}\text{Ni}$ ( $^{61}\text{Co}$ ),  $^{125}\text{Te}$ ( $^{125\text{m}}\text{Te}$ ),  $^{129}\text{I}$ ( $^{129}\text{Te}$ ,  $^{129\text{m}}\text{Te}$ ),  $^{161}\text{Dy}$ ( $^{161}\text{Tb}$ ),  $^{166}\text{Er}$ ( $^{166}\text{Ho}$ ),  $^{169}\text{Tm}$ ( $^{169}\text{Er}$ ),  $^{170}\text{Yb}$ ( $^{170}\text{Tm}$ ),  $^{197}\text{Au}$ ( $^{197}\text{Pt}$ ), etc.

The main purpose of this research is to develop effective Mössbauer sources for various isotopes and to apply this spectroscopy to many fields of researches. Among these researches, an improvement of  $^{166}\text{Er}$  Mössbauer spectroscopy is described in this report.

## EXPERIMENTS AND RESULTS:

Although several levels are known in the Mössbauer spectroscopy of Er, the 80.6 keV level of  $^{166}\text{Er}$  is the most useful level. Since the natural abundance of  $^{165}\text{Ho}$  is 100 %, by neutron irradiation of natural Ho,  $^{166}\text{Ho}$  with a half-life of 26.8 hours can be obtained for the Mössbauer source without by-product nuclides. As for the source material, we have synthesized  $\text{HoAl}_2$ , by arc-melting

method from Ho and Al. The obtained  $\text{HoAl}_2$  powder was sealed in polypropylene capsule with polystyrene resin. The neutron irradiation has been done by the pneumatic tube station(Pn) at KUR.

Since  $\text{HoAl}_2$  has a Curie temperature of about 25 K[1,2], the source temperature had better to be kept above 40 K to avoid line broadening by magnetic splitting. Since the recoilless fraction of Er compounds is low at high temperature, the sample and the source were usually cooled at the temperature of 40 K by using He-closed-cycle refrigerator. The gamma-rays with the energy of 80.6 keV have been measured by  $\text{CeBr}_3$  scintillation detector.

Until last year, several  $^{166}\text{Er}$  experiments have already been performed at KUR by users from other research groups[3]. However, because of the limitation from radiation safety regulations, the radioactivity of  $^{166}\text{Ho}$  was limited to 20 MBq. Some experiments had suffered from poor statistics. Therefore, in order to promote the  $^{166}\text{Er}$  experiments, we requested to extend the limitation and it was approved to be extended to 500 MBq.

In order to check the effectiveness of the gain of source activity and the radiation safety of experimental condition, a comparison was done using  $\text{Er}_2\text{O}_3$  absorber with the same source material of  $\text{HoAl}_2$  at about 18 to 20 K. The obtained activity was controlled by irradiation time. Similar measurements have been performed by 20 MBq and 98 MBq source as shown in Fig.1 and Fig.2, respectively. The experiment was successfully performed without any problem in radiation safety. The statistics of the spectra was well improved by the gain of radioactivity. The results showed the improvement of the  $^{166}\text{Ho}$  source was successful. The observed Mössbauer spectra showed the line broadening due to magnetic splitting of  $\text{HoAl}_2$  below Curie temperature. This source will be useful for various application in Er compounds, when measured at 40 K.

## REFERENCES:

- [1] E. Munck, D. Quitmann, S. Hufner, Z. Naturforsch. **21A**, 847 (1966).
- [2] E. Munck, D. Quitmann, S. Hufner, Phys. Lett. **24B**, 392 (1967).
- [3] S. Nakamura, H. Yokota, S. Kitao, Y. Kobayashi, M. Saito, R. Masuda, M. Seto, Hyperfine Interact. **240**, 75 (2019).

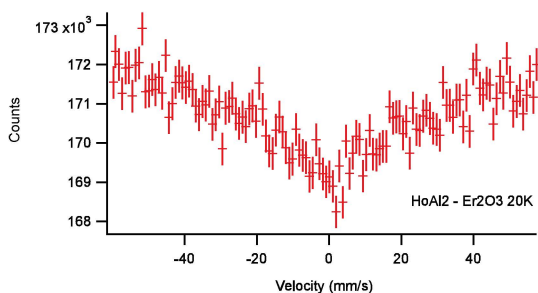


Fig. 1.  $^{166}\text{Er}$ -Mössbauer spectrum of  $\text{Er}_2\text{O}_3$  at 20 K using 20MBq  $^{166}\text{Ho}$  source in  $\text{HoAl}_2$ .

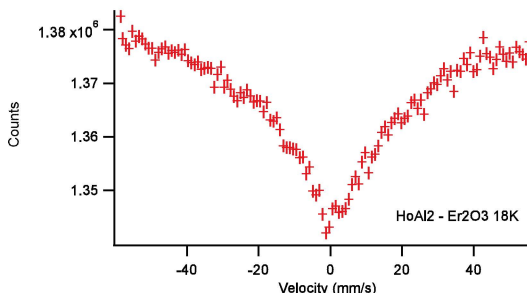


Fig. 2.  $^{166}\text{Er}$ -Mössbauer spectrum of  $\text{Er}_2\text{O}_3$  at 18 K using 98MBq  $^{166}\text{Ho}$  source in  $\text{HoAl}_2$ .